Research Square

Preprints are preliminary reports that have not undergone peer review.
They should not be considered conclusive, used to inform clinical practice,
or referenced by the media as validated information.

Deletion of fibroblast-derived CCN1 exacerbates renal fibrosis in mice

Shinji Sawai
Kyoto Prefectural University of Medicine
Tomohiro Nakata
Kyoto Prefectural University of Medicine
Atsushi Minamida
Kyoto Prefectural University of Medicine
Natsumi Mishima
Kyoto Prefectural University of Medicine
Hisaya Tanaka
Kyoto Prefectural University of Medicine
Ryo Kurose
Kyoto Prefectural University of Medicine
Erika Tsujinaka-Sawai
Kyoto Prefectural University of Medicine
Satomi Yamamoto
Kyoto Prefectural University of Medicine
Masashi Nakamura
Kyoto Prefectural University of Medicine
Minato Umehara
Kyoto Prefectural University of Medicine
Noriyuki Yamashita
Kyoto Prefectural University of Medicine
Yuhei Kirita
Kyoto Prefectural University of Medicine
Keiichi Tamagaki
Kyoto Prefectural University of Medicine
Naoki Nakagawa
Asahikawa Medical University
Satoaki Matoba
Kyoto Prefectural University of Medicine
Tetsuro Kusaba
kusaba@koto.kpu-m.ac.jp

Kyoto Prefectural University of Medicine

Article

Keywords: kidney fibrosis, fibroblast, epithelial cell, CCN1

Posted Date: November 13th, 2026

DOI: https://doi.org/10.21203/rs.3.rs-11442714/v1

License: This work is licensed under a Creative Commons Attribution 4.0 International License.
Read Full License

Additional Declarations: No competing interests reported.

Deletion of fibroblast-derived CCN1 exacerbates renal fibrosis in mice

Shinji Sawai[1], Tomohiro Nakata[1], Atsushi Minamida[1], Natsumi Mishima[1], Hisaya Tanaka[1], Ryo Kurose[1], Erika Tsujinaka-Sawai[1], Satomi Yamamoto[1], Masashi Nakamura[1], Minato Umehara[1], Noriyuki Yamashita[1], Yuhei Kirita[1], Keiichi Tamagaki[1], Naoki Nakagawa[2], Satoaki Matoba[3], and Tetsuro Kusaba[1, *]

[1] Department of Nephrology, Graduate School of Medical Science, Kyoto Prefectural University of Medicine, Kyoto, Japan

[2] Division of Cardiology and Nephrology, Department of Internal Medicine, Asahikawa Medical University, Asahikawa, Japan

[3] Department of Cardiovascular Medicine, Graduate School of Medical Science, Kyoto Prefectural University of Medicine, Kyoto, Japan

* Address correspondence to Tetsuro KUSABA,
Department of Nephrology, Graduate School of Medical Science, Kyoto Prefectural University of Medicine, 465 Kajii-cho, Kamigyo-ku, Kyoto, 602-8566, Japan
Tel.: +81-75-251-5511, Fax: +81-75-251-5514, E-mail: kusaba@koto.kpu-m.ac.jp

Running head: Fibroblast derived CCN1 and kidney fibrosis
Keywords: kidney fibrosis, fibroblast, epithelial cell, CCN1

Abstract

Chronic kidney disease is characterized by progressive renal fibrosis, yet effective anti-fibrotic therapies remain limited. Cellular Communication Network Factor 1 (CCN1) is a matricellular protein that regulates cell migration, proliferation, and extracellular matrix production. We previously demonstrated that proximal tubule-derived CCN1 promotes fibroblast recruitment and fibrosis during acute kidney injury; however, its role during progressive renal fibrosis remains unclear. Here, we investigated the cell source-specific functions of CCN1 using a unilateral ureteral obstruction (UUO) model and proximal tubule/fibroblast-specific CCN1-deficient mice. Proximal tubule-specific deletion of CCN1 did not alter renal fibrosis after UUO, whereas fibroblast-specific deletion unexpectedly exacerbated fibrosis and increased the expression of fibrotic markers. In vitro, CRISPR-Cas9-mediated CCN1 deletion in NRK49F fibroblasts markedly impaired cell migration and proliferation and increased cell size. RNA sequencing revealed downregulation of chemotaxis, PI3K-Akt, MAPK, focal adhesion, and TGF-β signaling pathways in CCN1 deleted NRK49F. Consistent with these findings, CCN1 deficiency reduced AKT and ERK phosphorylation and attenuated TGF-β-induced SMAD activation and expression of *Acta2* and *Ccn2*. In contrast, TGF-β-induced expression of extracellular matrix genes, including *Col1a1*, and *Fn1*, was enhanced by CCN1 deficiency, suggesting activation of alternative, SMAD-independent mechanisms. These findings indicate that fibroblast-derived CCN1 is not simply a pro-fibrotic factor but contributes to fibroblast integrity by maintaining their migratory and proliferative properties while modulating TGF-β signaling and extracellular matrix production. The biological effects of CCN1 are therefore highly dependent on its cellular source and the context of kidney injury.

Introduction

As the population ages, the number of patients with chronic kidney disease (CKD) is increasing worldwide, posing a significant societal burden [1]. A characteristic histological feature of CKD is the progressive replacement of normal renal parenchyma with fibrotic tissue, accompanied by persistent inflammation and ultimately leading to loss of renal function[2, 3]. The development of renal fibrosis involves extensive intercellular communication among multiple cell types through numerous cytokines and growth factors acting in both paracrine and autocrine manners [4]. Although transforming growth factor-β (TGF-β) and connective tissue growth factor (CTGF) are well-established mediators of renal fibrosis, therapeutic strategies targeting these pathways have not demonstrated sufficient efficacy in clinical or preclinical trials [4]. Therefore, a deeper understanding of the molecular mechanisms underlying renal fibrosis is needed to develop more effective therapies for CKD.

During renal injury, fibrosis is promoted through interactions between injured tubular epithelial cells and surrounding fibroblasts [5]. Cytokines and growth factors, including TGF-β, platelet-derived growth factor (PDGF), and CTGF, released from injured tubules are well-known mediators of this intercellular communication [5-10]. We recently demonstrated that Cellular Communication Network Factor 1 (CCN1), secreted by tubular epithelial cells during the acute phase of kidney injury, recruits fibroblasts to sites of inflammation and promotes fibrosis [11, 12]. CCN1 belongs to the CCN family of matricellular proteins and, through interactions with integrins, regulates the migration and proliferation of various cell types, including fibroblasts, via activation of ERK [13]. The role of CCN1 in tissue injury and fibrosis has been investigated in multiple organs and disease models[13, 14]. However, the role of CCN1 on tissue fibrosis development is not straight forward. For example, opposite results of the effects of CCN1 on liver fibrosis has been proposed [15-17]. Regarding kidney, neutralization of CCN1 has also been shown to ameliorate kidney injury [18]. Thus, the biological effects of CCN1 appear to vary across tissues and pathological conditions, highlighting the complexity of CCN1 signaling.

CCN1 is expressed in the kidney not only by tubular epithelial cells but also by podocytes and vascular cells [19]. Although our previous studies have elucidated the role of tubular epithelial cell-derived CCN1 during acute kidney injury [11], its contribution to chronic and progressive renal fibrosis remains unclear. In the

present study, we used unilateral ureteral obstruction (UUO), a well-established model of progressive renal fibrosis, to investigate the role of proximal tubule-derived CCN1 in chronic kidney injury. In addition, because fibroblasts themselves can secrete CCN1 [20], we investigated the role of fibroblast-derived CCN1 in progressive renal fibrosis. By examining these distinct cellular sources of CCN1, we sought to clarify the cell source-specific functions of CCN1 in renal fibrosis.

Methods

Mouse Experiments

We used mice carrying a CreERT2 cassette at the SLC34a1 locus, allowing tamoxifen-inducible expression of Cre recombinase in proximal tubular epithelial cells. These mice (SLC34a1GCE) were crossed with R26tdTomato reporter mice, in which tdTomato expression is induced following Cre-mediated excision of a floxed STOP cassette [21]. This genetic strategy enabled specific labeling of proximal tubular epithelial cells with tdTomato following tamoxifen administration. To generate mice with inducible tubular epithelial cell-specific deletion of CCN1 (PT-CCN1-KO), SLC34a1GCE;R26tdTomato mice were further crossed with mice homozygous for the floxed Ccn1 allele. Experiments were performed using male mice aged 8–10 weeks. Littermates were randomly assigned to the experimental groups.

We generated fibroblast-specific CCN1 knockout mice (Fib-CCN1-KO) by crossing Pdgfrb;R26tdTomatoCreERT2 mice (PDGFRβCE) [22], kindly provided by Professor Naoki Nakagawa (Asahikawa Medical University, Japan), with mice homozygous for the floxed Ccn1 allele. Experiments were performed using male mice aged 8–15 weeks. Littermates were randomly assigned to the experimental groups.

For genetic recombination, tamoxifen (Sigma-Aldrich, St. Louis, MO, USA) was dissolved in 3% (vol/vol) ethanol containing peanut oil (Sigma-Aldrich, St. Louis, MO, USA). Tamoxifen was administered by intraperitoneal injection at a dose of 3 mg per mouse once daily for five consecutive days.

UUO mouse model was generated as described previously [23]. Mice were anesthetized with isoflurane and placed in the prone position while their body temperature was maintained using a heating pad throughout the procedure. The right ureter was exposed through a small dorsal incision and ligated at two sites in its midportion using 5-0 silk sutures. Mice were sacrificed at 1, 7, or 14 days after surgery, and both the obstructed and contralateral kidneys were harvested for subsequent analyses.

Mice were housed under specific pathogen-free conditions at 25℃ with a 12h light/dark cycle and had ad libitum access to standard chow and water. All animal experiments were approved by the Animal Experiment Committee of Kyoto Prefectural University of Medicine and were conducted in accordance with institutional regulations and the Guidelines for Proper Conduct of Animal Experiments issued by the Science Council of Japan.

Tissue preparation and histological analysis

At the indicated time points, mice were anesthetized with 5% (vol/vol) isoflurane (FUJIFILM Wako Pure Chemical Corporation, Osaka, Japan; Cat. No. 099-06571) using an animal anesthesia vaporizer (SHIN-EI INDUSTRIES, INC., Japan; product code: 200193223). Isoflurane administration was maintained at 5% throughout the procedure until kidney collection. Under anesthesia, laparotomy and bilateral thoracotomy were performed, followed by transcardial perfusion with physiological saline. Cessation of cardiac and respiratory activity was visually confirmed before kidney collection. The kidneys were then harvested and divided into portions according to the intended downstream analyses.

For frozen section preparation, kidney tissues were fixed in 4% paraformaldehyde (Fujifilm Wako Pure Chemical Corporation, Osaka, Japan) on ice for 1 h, followed by overnight immersion in 30% (vol/vol) sucrose in PBS at 4℃. The tissues were then embedded in optimal cutting temperature (OCT) compound (Sakura Finetek Japan Co., Ltd., Tokyo, Japan) and sectioned at a thickness of 7μm.

For paraffin section preparation, kidney tissues were fixed in 4% paraformaldehyde and subsequently processed for paraffin embedding by Applied Medical Research Laboratory (Osaka, Japan). Paraffin-embedded tissues were sectioned at a thickness of 4μm. Periodic acid–Schiff (PAS) and Picro-Sirius Red staining were performed using standard procedures.

For histological assessment of mouse kidney samples, the extent of interstitial fibrosis was semi-quantitatively evaluated in Picro-Sirius Red-stained sections. Five randomly selected fields per kidney were imaged at ×200 magnification using a BZ-X800 microscope (Keyence Corporation, Osaka, Japan). The proportion of the interstitial area exhibiting positive Picro-Sirius Red staining was scored as follows: 0, 0%; 1, 1–10%; 2, 11–25%; 3, 26–50%; 4, 51–75%; and 5, 76–100%. [11, 24]

Isolation of tdTomato-positive proximal tubular epithelial cells and fibroblasts by FACS

tdTomato-positive proximal tubular epithelial cells and fibroblasts were isolated by fluorescence-activated cell sorting (FACS) from SLC34a1GCE;R26tdTomato mice and Pdgfrb;R26tdTomato CreERT2 mice, respectively, as previously described [11, 25]. Briefly, the renal cortex was finely minced and enzymatically

dissociated with Liberase TL Research Grade (Roche; Sigma-Aldrich, St. Louis, MO, USA) and DNase inhibitor (60 U/mL; Sigma-Aldrich, St. Louis, MO, USA) at 37°C for 30 min to generate a single-cell suspension. The cell suspension was washed twice with PBS and sequentially passed through 70- and 40-μm cell strainers (Corning Incorporated, Corning, NY, USA). Cells were then resuspended in PBS containing 10% FBS (NACALAI TESQUE, INC., Kyoto, Japan) and DAPI (2 mg/mL, 1:500, FUJIFILM Wako Pure Chemical Corporation, Osaka, Japan) and subjected to FACS using an MA900 Cell Sorter (Sony, Tokyo, Japan). DAPI-positive dead cells were excluded during sorting. tdTomato-positive, DAPI-negative cells isolated from SLC34a1GCE;R26tdTomato mice and Pdgfrb;R26tdTomato CreERT2 mice were collected as proximal tubular epithelial cells and fibroblasts, respectively, in DMEM (FUJIFILM Wako Pure Chemical Corporation, Osaka, Japan) supplemented with 10% FBS.

Immunofluorescence analysis

For immunofluorescence staining, samples were blocked with 3% bovine serum albumin (BSA; NACALAI TESQUE, INC., Kyoto, Japan) in PBS and incubated with the primary antibodies listed in Supplementary Table S1 overnight at 4 °C. After washing, samples were incubated with the appropriate fluorophore-conjugated secondary antibodies listed in Supplementary Table S1 for 1 h at room temperature. Nuclei were counterstained with DAPI or DRAQ5 (BioStatus, Leicestershire, UK; 1:200), followed by mounting with ProLong Gold Antifade Mountant (Thermo Fisher Scientific, Waltham, MA, USA). Fluorescence images were acquired using an FV1000 confocal microscope (Olympus Corporation, Tokyo, Japan) or an LSM 900 confocal microscope (Carl Zeiss Microscopy GmbH, Jena, Germany).

Cell culture and treatment

Normal rat kidney fibroblasts (NRK49F) were obtained from the JCRB Cell Bank (Japanese Collection of Research Bioresources Cell Bank, Osaka, Japan). Cells were maintained in DMEM (FUJIFILM Wako Pure Chemical Corporation, Osaka, Japan) supplemented with 5% fetal bovine serum (FBS; NACALAI TESQUE, INC., Kyoto, Japan) and 1% penicillin-streptomycin (FUJIFILM Wako Pure Chemical Corporation, Osaka, Japan) and cultured at 37℃ in a humidified atmosphere containing 5% CO_2.

For experiments involving protein or RNA extraction, NRK49F cells were cultured

on dishes precoated with 0.1% gelatin (Cosmo Bio, Tokyo, Japan). Gelatin coating was performed according to the manufacturer's instructions.

For stimulation experiments, NRK49F cells were treated with human recombinant CCN1 (2 μg/mL; PeproTech) or control medium for 30 min before Western blot analysis. For TGF-β stimulation, cells were treated with TGF-β (10 ng/mL; PeproTech) or control medium for 1 h before Western blot analysis or for 24 h before qPCR analysis.

Generation of CCN1-deficient NRK49F cells using CRISPR-Cas9

CCN1-deficient NRK49F cells were generated using a CRISPR-Cas9 system as previously described [11]. Briefly, NRK49F cells were transduced with a pLentiCRISPR v2-based lentivirus encoding Cas9, puromycin resistance, and an sgRNA targeting exon 2 of the rat Ccn1 gene (GGAGGCGCCCAAGTGCGCCC; PAM, CGG). The lentiviral construct carrying this sgRNA was generated using the same procedure as previously described. Twenty-four hours after transduction, puromycin was added to the culture medium to select transduced cells. After 48 h of selection, puromycin was removed, and the surviving cells were cultured for an additional 4 days. Single-cell clones were subsequently established by limiting dilution. Individual colonies derived from single cells were isolated using cloning rings and expanded in 6-well plates. Loss of CCN1 protein expression was confirmed by Western blotting using antibodies against CCN1 and GAPDH.

Single-cell migration assay

For the single-cell migration assay, NRK49F cells were seeded in 6-well plates. After allowing the cells to adhere for several hours, they were treated with mitomycin C (3 μg/mL; FUJIFILM Wako Pure Chemical Corporation, Osaka, Japan) for 1 h to inhibit cell proliferation. The cells were then washed twice with PBS, and the medium was replaced with fresh culture medium. For live-cell imaging, individual cells were monitored every 10 min for 24 h using a JuLI™ Stage Cell History Recorder (NanoEntek, Seoul, Korea). Cell trajectories were tracked using the TrackMate plugin in ImageJ, and the mean cumulative migration distance of NRK49F cells was calculated.

Proliferation assay

NRK49F cells were seeded in 96-well plates at a density of 1×10^3 cells per well.

Cell numbers were determined using a TC20™ Automated Cell Counter (Bio-Rad, Japan) based on the trypan blue dye exclusion method. After overnight culture, the medium was replaced with fresh culture medium. After an additional 24 h, the number of viable cells in each well was assessed using the Premix WST-1 Cell Proliferation Assay System (Takara Bio, Shiga, Japan) according to the manufacturer's instructions.

Western blot analysis

Whole-cell lysates were prepared using RIPA buffer on ice. Protein samples were denatured by heating at 95℃ for 5 min and separated by SDS-PAGE, followed by transfer onto polyvinylidene difluoride (PVDF) membranes (Immobilon-P, IPVH00010; Millipore, MA, USA). After blocking with either 5% nonfat dry milk or 3% bovine serum albumin (BSA) in TBS containing 0.1% Tween 20 (TBS-T) for 1 h at room temperature, the membranes were incubated overnight at 4℃ with the appropriate primary antibodies listed in Supplementary Table S2. After washing with TBS-T, the membranes were incubated with the corresponding secondary antibodies listed in Supplementary Table S2. Chemiluminescent signals were detected using Clarity or Clarity Max Western ECL Substrate (Bio-Rad Laboratories, Hercules, CA, USA). Band intensities were quantified using ImageJ software (National Institutes of Health, Bethesda, MD, USA).

RNA extraction and real-time quantitative PCR

Total RNA was extracted from the renal cortex, FACS-sorted cells, or NRK49F cells using the NucleoSpin® RNA kit (Macherey-Nagel, Düren, Germany). A total of 200 ng of RNA was reverse-transcribed into cDNA using PrimeScript™ RT Master Mix (Takara Bio, Shiga, Japan). Real-time quantitative PCR was performed using KAPA SYBR FAST qPCR Master Mix (2×) Universal (Kapa Biosystems, Wilmington, MA, USA) on a Thermal Cycler Dice Real Time System (Takara Bio, Shiga, Japan). Gene expression levels were normalized to β-actin for mouse samples and GAPDH for NRK49F cells. Primer sequences are provided in Supplementary Table S3.

RNA sequencing

RNA samples were submitted to the NGS Core Facility at the Research Institute for Microbial Diseases, Osaka University, for library preparation and sequencing. Libraries were prepared using the TruSeq Stranded mRNA Sample Preparation

Kit (Illumina, San Diego, CA, USA) according to the manufacturer's instructions. Sequencing reads were aligned to the rat reference genome using STAR version 2.7.10a. Uniquely mapped reads were quantified using the featureCounts function of the Subread package.

Bioinformatic analysis

Data were analyzed using R software version 4.3.2 (https://www.R-project.org/). The edgeR package was used for a differential expression analysis36. Genes with p value < 0.05 and an absolute log2 fold change > 1 were considered to be significant differentially expressed genes. The fgsea package was used for a gene set enrichment analysis. We used pheatmap package to generate the heatmap.

Statistical analysis

Data are presented as the mean ± standard error of the mean (SEM). Comparisons between two independent groups were performed using an unpaired Student's t-test, whereas paired data were analyzed using a paired Student's t-test. Comparisons among multiple groups were performed using one-way or two-way ANOVA, as appropriate, followed by Dunnett's multiple-comparisons test. Statistical analyses were performed using GraphPad Prism. A P value < 0.05 was considered statistically significant. Details of the statistical tests used for individual experiments are provided in the corresponding figure legends.

Results

Deletion of proximal tubule-derived CCN1 does not affect the kidney fibrosis

We first examined whether proximal tubule (PT)-derived CCN1 mitigates kidney fibrosis using the UUO model, an extensive kidney fibrosis model, together with tubule-specific CCN1 knockout (KO) mice (hereafter, homozygous mutants are referred to as PT-CCN1-KO) (Fig. 1A). To directly confirm CCN1 deletion in PT cells, we generated trigenic mice carrying Slc34a1-GCE and R26-tdTomato alleles, with or without PT-CCN1-KO. Following selective labeling of PT cells, mice underwent UUO and were sacrificed 14 days later (Fig. 1A). Immunofluorescence analysis demonstrated that PT cells were labeled with tdTomato, and no tdTomato+ cells were positive for PDGF receptor-β (PDGFRβ), indicating that tubular epithelial cells did not transition into interstitial mesenchymal cells (Fig. 1B). RT-PCR on sorted tdTomato+ tubular epithelial cells demonstrated loss of *Ccn1* expression in the PT of PT-CCN1-KO mice (Fig. 1C, 1D).

We next analyzed the effect of PT-specific deletion of CCN1 on kidney fibrosis. At 14 days after UUO, Sirius Red staining showed extensive tissue fibrosis, but there was no difference between WT and PT-CCN1-KO mice (Fig. 1E, 1F). qPCR analysis demonstrated no significant differences in the expression of markers for tubular injury (*Havcr1*), tubular integrity (*Lrp2*), pro-inflammatory and profibrotic cytokines (*Ccl2*, *Tgfb1*), macrophage (*Cd68*), and fibrosis (*Acta2*, *Col1a1*, *Fn1*) between WT and PT-CCN1-KO mice (Fig. 1G).

Deletion of fibroblast-derived CCN1 promotes the kidney fibrosis

To investigate why tubule-specific CCN1-KO had no effect on fibrosis, we analyzed changes in gene expression of *Ccn1* over time using whole-tissue PCR. There was no difference in *Ccn1* expression between was PT-CCN1-KO and WT mice at day 14 (Fig. 2A), indicating that PT cells is not a major source of CCN1 at chronic phase after UUO.

To explore the localization of CCN1 expression in other than PT cells of the injured kidney, we analyzed single-cell transcriptome profiling datasets from UUO kidneys [26], obtained from the Kidney Interactive Transcriptomics database (http://humphreyslab.com/SingleCell/). We found a time-dependent increase in *Ccn1* expression in UUO kidneys, which was localized not only to PT cells but also to fibroblasts (Fig. 2B). These findings suggest that CCN1 is

upregulated in damaged tubules during acute kidney injury, and that in more extensive fibrosis models such as UUO, fibroblast-derived CCN1 may also contribute to fibrosis.

Therefore, we next investigated the effect of fibroblast-specific CCN1 deletion on renal fibrosis, using fibroblast-specific CCN1-KO mice (hereafter, homozygous mutants are referred to as Fib-CCN1-KO) (Fig. 3A). To directly confirm CCN1 deletion in fibroblasts, we generated trigenic mice carrying PDGFRβCE and R26-tdTomato alleles, with or without Fib-CCN1-KO. Following selective labeling of PDGFRβ+ cells, mice underwent UUO and were sacrificed 14 days later (Fig. 3A). Immunofluorescence analysis demonstrated that interstitial PDGFRβ+ cells were labeled with tdTomato (Fig. 3B). RT-PCR on sorted tdTomato+ fibroblasts demonstrated loss of Ccn1 expression in Fib-CCN1-KO mice (Fig. 3C, 3D).

We then assessed the effect of fibroblast-specific CCN1 deletion on renal fibrosis. At 14 days after UUO, Sirius Red staining showed that tissue fibrosis was not improved but rather became more prominent in Fib-CCN1-KO mice (Fig. 3E, 3F). qPCR analysis demonstrated that some fibrosis markers (*Acta2* and *Fn1*) were increased in Fib-CCN1-KO mice (Fig. 3G).

Gene deletion of CCN1 promote cellular hypertrophy in fibroblasts

To gain further mechanistic insight, we generated CCN1-KO NRK49F cells, a fibroblast cell line, using CRISPR-Cas9-based gene editing. We targeted exon 2 for gene editing, as it precedes the sequence encoding the integrin-binding site (Fig. 4A). We isolated single-cell-derived clones in which CCN1 expression was undetectable (Fig. 4A, 4B, 4C). Microscopic examination showed that CCN1-KO NRK49F cells were enlarged (Fig. 4D), and quantification confirmed a marked increase in cell size in CCN1-KO NRK49F cells (Fig. 4E).

We next examined transcriptomic differences between NRK49F cells with and without CCN1-KO using RNA-seq. Unsupervised analysis of gene expression by principal component analysis (PCA) revealed that the transcriptional landscapes of CCN1-KO and control NRK49F cells formed independent clusters, indicating distinct gene expression patterns (Fig. 5A). Comparison of CCN1-KO and control NRK49F cells identified 442 upregulated and 373 downregulated genes among 14,659 genes analyzed, which exhibited significant differential expression (false discovery rate [FDR]-corrected p-value < 0.1, absolute fold change > 2) (Fig. 5B). Gene Ontology (GO) Biological Process

analysis revealed that terms related to chemotaxis were downregulated in CCN1-KO NRK49F cells (Fig. 5C, 5D). KEGG pathway analysis identified several significantly enriched, downregulated pathways, including the PI3K-Akt signaling pathway, the MAPK pathway, focal adhesion, and the TGF-β signaling pathway (Fig. 5E, 5F).

Gene deletion of CCN1 reduced proliferation and migration

We next analyzed the molecular phenotypes of CCN1-KO NRK49F cells identified by transcriptomic analysis. Cell proliferation was markedly decreased in CCN1-KO NRK49F cells (Fig 6A). A single-cell migration assay revealed that the migration distance was decreased in CCN1-KO NRK49F cells (Fig 6B). Western blotting showed a marked decrease in the phosphorylation of AKT and ERK, consistent with the transcriptomic results (Fig 6C, 6D). Given the reduced TGF-β signaling suggested by transcriptomics, qPCR analysis showed that *Acta2* and *Ccn2* expression was reduced in CCN1-KO NRK49F cells (Fig 7A). Regarding extracellular matrix components, *Col1a1* expression was upregulated in CCN1-KO NRK49F cells, whereas no differences were observed in *Fn1* expression (Fig 7A). After TGF-β treatment, *Col1a1*, and *Fn1* were upregulated in both CCN1-KO and control NRK49F cells, but the upregulation was much more prominent in CCN1-KO NRK49F cells (Fig 7A). In contrast, *Acta2* and *Ccn2* were also upregulated by TGF-β treatment, however, the upregulation was much less in CCN1-KO NRK49F cells. Finally, we analyzed SMAD phosphorylation, a major transcription factor downstream of TGF-β signaling. At baseline, there was no difference in SMAD phosphorylation between control and CCN1-KO NRK49F cells (Fig 7B, 7C). TGF-β enhanced SMAD phosphorylation in control NRK49F cells, but this increase was diminished in CCN1-KO NRK49F cells (Fig 7B, 7C).

Discussion

Histologically, CKD is characterized by the loss of normal renal parenchyma, which is progressively replaced by fibrotic tissue, ultimately resulting in loss of renal function. The development of renal fibrosis involves extensive intercellular communication among various cell types through numerous cytokines and growth factors, acting in both paracrine and autocrine manners [4]. In this study, we investigated the mechanisms by which CCN1, particularly fibroblast-derived CCN1, affects renal fibrosis. We demonstrated that deletion of tubule-derived CCN1 did not affect the development of chronic kidney fibrosis. In contrast, and contrary to our initial expectation, deletion of fibroblast-derived CCN1 exacerbated tissue fibrosis. In NRK-49F cells, deletion of CCN1 resulted in the loss of fundamental fibroblast properties, including migratory and proliferative capacities. Although attenuation of SMAD-mediated TGF-β signaling was observed, TGF-β-induced extracellular matrix (ECM) production was paradoxically enhanced. These findings suggest that CCN1 contributes to the maintenance of fibroblast integrity and that its loss suppresses SMAD-dependent signaling while promoting alternative pathways of ECM production.

In this study, we examined the effects of inhibiting CCN1 derived from both PTs and fibroblasts; however, neither approach improved fibrosis in the UUO model. Previous studies using neutralizing antibodies against CCN1 have demonstrated an improvement in IRI-induced kidney injury, but whether CCN1 inhibition exerts anti-fibrotic effects during the chronic phase of UUO remains unclear, suggesting that the effects of CCN1 may be context-dependent [18, 27]. Consistent with this notion, in our previous studies using PT-specific CCN1-KO mice, fibrosis associated with IRI was attenuated, whereas fibrosis following cisplatin-induced kidney injury was not [11, 12]. More recently, Zhang et.al. demonstrated that renal tubular epithelial cell-specific CCN1 knockdown did not improved, rather exacerbated IRI through inhibiting macrophage infiltration which can contribute tubular repair[28]. These findings suggest that the anti-fibrotic effects of PT-derived CCN1 inhibition may vary depending on the type and severity of kidney injury. Furthermore, inhibition of CCN1 from only one cellular source, either PTs or fibroblasts, may allow compensatory CCN1 expression from other cell types during kidney injury, resulting in insufficient suppression of tissue CCN1 levels. In addition, CCN1 derived from injured PTs and fibroblasts may exert distinct biological effects. Therefore, targeting CCN1 as an anti-fibrotic therapy may be challenging, particularly through systemic pharmacological inhibition, and further

elucidation of the context-dependent and cell source-specific functions of CCN1 is required.

Since CCN1 was first identified as a molecule rapidly secreted by fibroblasts in response to serum or PDGF stimulation [20], it is important to examine the role of fibroblast-derived CCN1 in tissue fibrosis. Although our study is the first to investigate fibroblast-specific CCN1 inhibition in the kidney, studies in other organs have reported diverse effects. In the heart, fibroblast-specific CCN1 knockout suppresses scar formation following myocardial infarction but results in structural instability and increased mortality [29]. More recent report showed that cardiac fibroblast-specific CCN1 deletion ameliorated cardiac dysfunction in a dilated cardiomyopathy model [30]. In the skin, analysis of fibroblast-specific CCN1-KO mice showed reduced collagen accumulation in bleomycin-induced skin lesions, whereas collagen accumulation was enhanced during the chronic phase of a wound-healing model [31]. In cancer tissues, deletion of CCN1 in cancer-associated fibroblasts suppresses neovascularization, thereby promoting fibrosis while inhibiting cancer metastasis [32]. In our study, however, fibroblast-specific CCN1 knockout failed to suppress fibrosis in the UUO model.

One possible explanation is the relatively low proportion of fibroblasts among the cells comprising the kidney compared with tissues such as the skin. In addition, the mechanisms underlying fibrosis differ substantially among these models. In fibrosis models involving acute tissue injury, such as skin injury and myocardial infarction, the loss of tissue is rapidly followed by its replacement with scar tissue. In contrast, UUO induces a more gradual loss of renal parenchyma accompanied by progressive replacement with fibrous tissue. These differences in the nature and temporal progression of fibrosis may have influenced the extent to which fibroblast-derived CCN1 contributes to fibrogenesis and, consequently, the effect of fibroblast-specific CCN1 deletion on fibrosis. Furthermore, unlike tissues in which fibroblasts constitute a relatively large proportion of the cellular population, the kidney produces substantial amounts of CCN1 from tubular epithelial cells. Thus, compensatory CCN1 production from tubular epithelial cells may have masked the effect of fibroblast-specific CCN1 deletion in the UUO model.

In our in vitro study, CCN1 knockout in fibroblasts markedly reduced cell motility, accompanied by decreased cell proliferation and a consequent increase in cell volume. Previous in vitro studies have shown that suppression of CCN1 expression in smooth muscle cells (SMCs) using siRNA markedly reduces

fibroblast migration, consistent with our findings [33]. Our RNA-seq and protein expression analyses revealed a modest reduction in ERK and AKT phosphorylation; however, these findings do not fully align with previous reports. In addition, our study demonstrated that CCN1 knockout also inhibited fibroblast proliferation. Taken together, these findings suggest that CCN1 plays an important role in fibroblast migration and proliferation and may also contribute to the maintenance of fibroblast integrity through both autocrine and paracrine mechanisms.

Furthermore, RNA-seq analysis revealed that CCN1-KO attenuated TGF-β signaling, and Western blot analysis confirmed reduced SMAD activation following TGF-β stimulation, accompanied by decreased expression of its canonical target genes, *Acta2* and *Ccn2*. Previous studies have shown that siRNA-mediated inhibition of CCN1 suppresses SMAD3 phosphorylation and attenuates TGF-β signaling [34]. Together with our findings, these results support the notion that CCN1 positively regulates the TGF-β–SMAD pathway. In contrast, the TGF-β-induced upregulation of *Col1a1*, and *Fn1* was enhanced in CCN1-KO fibroblasts. It is well established that *Col1a1* expression can also be regulated through SMAD-independent pathways [35]. These findings suggest that, although CCN1 deficiency suppresses the SMAD-dependent induction of *Acta2* and *Ccn2*, the expression of *Col1a1*, *Fn1*, and other extracellular matrix-related genes may be enhanced through alternative or SMAD-independent mechanisms. The intracellular signaling pathways underlying these differential responses remain largely unclear and warrant further investigation.

Our study has several limitations. First, although CCN1 is secreted into the extracellular space and is thought to exert its effects through autocrine and paracrine mechanisms, we cannot exclude the possibility that CCN1 also has intracellular functions. Second, CCN1 has been reported to promote the migration of inflammatory and vascular cells [36-39]; however, these effects were only examined by qPCR in the present study. Thus, altered recruitment or behavior of these cell populations may have contributed to the exacerbation of fibrosis observed in the Fib-CCN1-KO model. Finally, although we demonstrated that CCN1 deficiency suppresses TGF-β–SMAD signaling, the molecular mechanism underlying this effect remains unclear. Further studies are therefore required to determine how CCN1 regulates intracellular signaling in fibroblasts and how its effects on other cell populations contribute to renal fibrosis.

In conclusion, neither tubule-specific nor fibroblast-specific inhibition of

CCN1 improved tissue injury or fibrosis in the UUO model of progressive renal fibrosis. These findings suggest that cell type-specific inhibition of CCN1 alone is insufficient to suppress renal fibrosis, potentially because of compensatory CCN1 expression by other cell types. Our in vitro findings further indicate that CCN1 is not simply a pro-fibrotic factor in fibroblasts but contributes to the maintenance of fibroblast homeostasis, including their migratory and proliferative capacities. Thus, the biological effects of CCN1 appear to be highly dependent on the cellular source and the context, timing, and severity of tissue injury. Collectively, our findings provide new insights into the complex and cell source-specific functions of CCN1 in progressive kidney fibrosis.

Data availability

RNA-seq data for all samples were deposited in the Gene Expression Omnibus under the accession number GSE351150. Secure token for reviewer access: wdqbkywmnbqrlgp.

Data sharing statement

The data supporting the findings of this study are available in the main manuscriptl. In addition, we will share models, protocols, methods, and other useful materials and resources related to the article as far as possible.

Author contributions

S.S. T.N, and T. K. designed the study, performed the experiments, analyzed the data, and wrote the manuscript. A.M. performed the experiments. Y.K. analyzed the data. N.M., E.T-S., R.K., H.T., S.Y., M.N., M.U., N.Y., K.T., N.N., and, S.M. contributed to the discussion.

Disclosure

The authors declare no conflict of interest associated with this study.

Funding

The authors received no specific funding for this work.

Acknowledgments:

The authors would like to thank Prof. Lester F. Lau for his kind gift of CCN1-floxed mice.

Figures

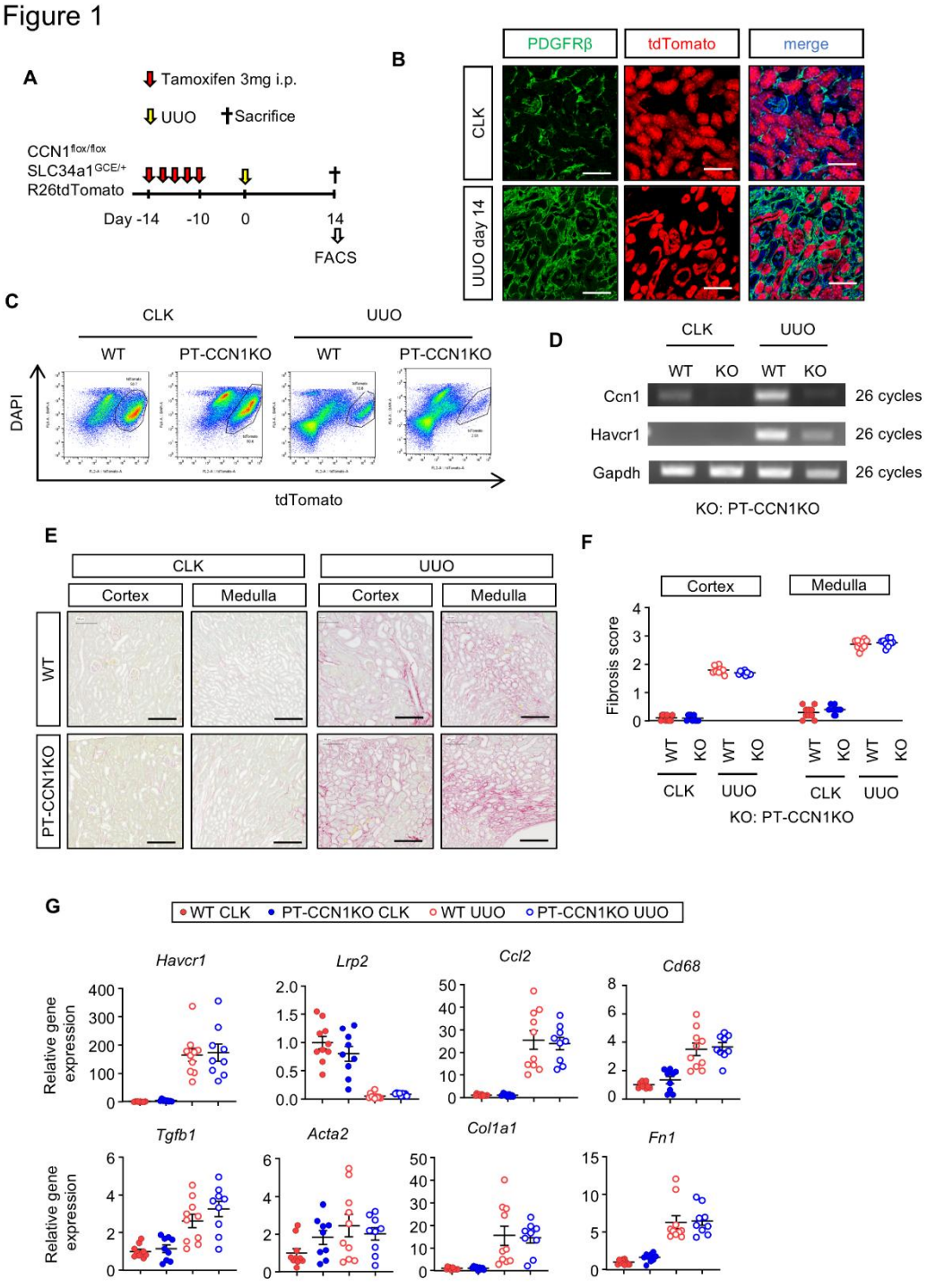


Fig. 1 Proximal tubule-specific deletion of CCN1 does not promote tissue fibrosis in UUO

(A) Experimental scheme. Proximal tubular-specific CCN1 knockout mice (CCN1Flox/Flox SLC34a1GCE x R26tdTomato: PT-CCN1-KO) received UUO

and tamoxifen (3 mg/kg at each time point) as indicated. (B) Representative immunofluorescence images of tdTomato and PDFGRβ in PT-CCN1-KO mice. (C) Isolation of tdTomato+ tubular epithelial cells using FACS. (D) RT-PCR of the *Ccn1* genes in sorted tdTomato+ tubular epithelial cells. (E). Representative images of Sirius-red staining. (F) Semi-quantitative fibrosis scores at 14 days after UUO. (G) qPCR of RNA from whole kidneys as representative markers of tubular injury (*Havcr1*), tubular integrity (*Lrp2*), chemokine (*Ccl2*), myofibroblasts (*Acta2*), extracellular matrix (*Col1a1* and *Fn1*), macrophages (*Cd68*) and profibrotic factor (*Tgfb1*). The scale bars indicate 50 μm in (B), and (E). For all groups, data are means ± SEM. Statistical analyses were performed by paired t-test for comparisons of IRI kidney and CLK and by ANOVA and Dunnett's post hoc test for comparisons of multiple variables. *P < 0.05.

Figure 2

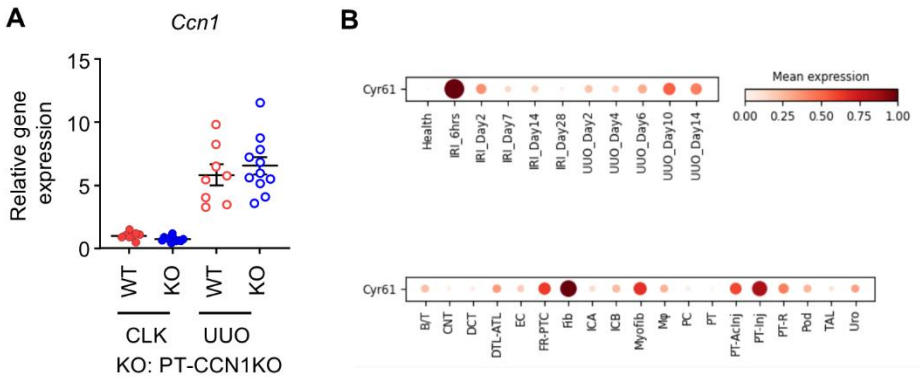
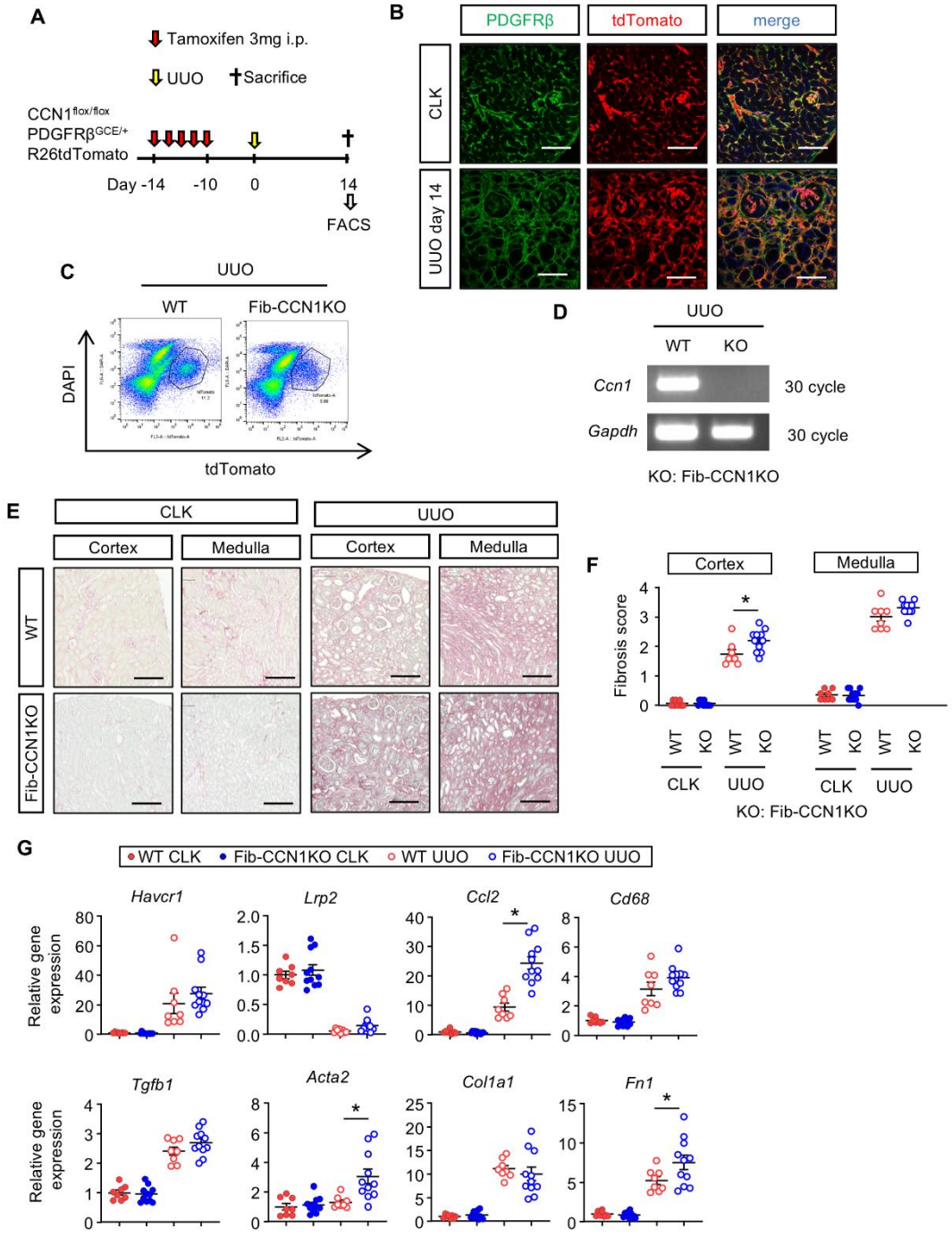


Fig2 CCN1 is upregulated during renal fibrogenesis–induced by UUO

(A) qPCR of RNA from the whole kidney for *Ccn1*. (B) The distribution and relative expression of *Ccn1* in different renal cell types of the UUO kidneys from single-nucleus RNA sequencing analysis (http://humphreyslab.com/SingleCell/). Statistical analyses were performed by paired t-test for comparisons of IRI kidney and CLK and by ANOVA and Dunnett's post hoc test for comparisons of multiple variables.

Figure 3

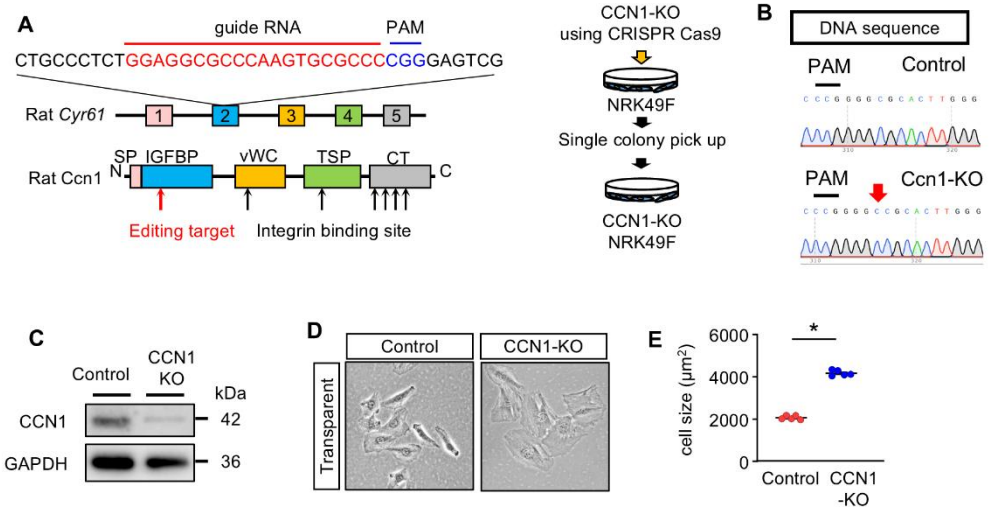


570 **Fig3 Fibroblasts specific deletion of CCN1 exacerbates tissue fibrosis in**
571 **UUO**

572 (A) Experimental scheme. Fibroblast-specific CCN1 knockout mice
573 (CCN1Flox/Flox PDGFRβCE x R26tdTomato: Fib-CCN-KO) received UUO and
574 tamoxifen (3 mg/kg at each time point) as indicated. (B) Representative

immunofluorescence images of tdTomato and PDFGRβ in mice with or without UUO. (C) Isolation of tdTomato+ fibroblasts using FACS. (D) RT-PCR of the *Ccn1* gene in sorted tdTomato+ fibroblasts. (E). Representative images of Sirius-red staining. (F) Semi-quantitative fibrosis scores at 14 days after UUO. (G) qPCR of RNA from whole kidneys as representative markers of tubular injury (*Havcr1*), tubular integrity (*Lrp2*), chemokine (*Ccl2*), myofibroblasts (*Acta2*), extracellular matrix (*Col1a1* and *Fn1*), macrophages (*Cd68*), and profibrotic factor (*Tgfb1*). The scale bars indicate 50 μm in (B), and (E). For all groups, data are means ± SEM. Statistical analyses were performed by paired t-test for comparisons of IRI kidney and CLK and by ANOVA and Dunnett's post hoc test for comparisons of multiple variables. *P < 0.05.

Figure 4



588 **Fig 4 Establishment of CCN1 deficient fibroblasts**

589 (A) Schematic illustration of the targeting strategy for the knockout of CCN1 in
590 NRK49F by the CRISPR cas9 system. (B) DNA sequence result indicates a
591 single base (Cytosine) is inserted (red arrow). (C) Western blot analysis of CCN1
592 in the cell lysate of CCN1-KO NRK49F. (D) Representative transparent pictures
593 of CCN1-KO NRK49F. (E) Quantification of Cell size. For all groups, data are
594 means ± SEM. Statistical analyses were performed by paired t-test for
595 comparisons. *P < 0.05.
596
597

Figure 5

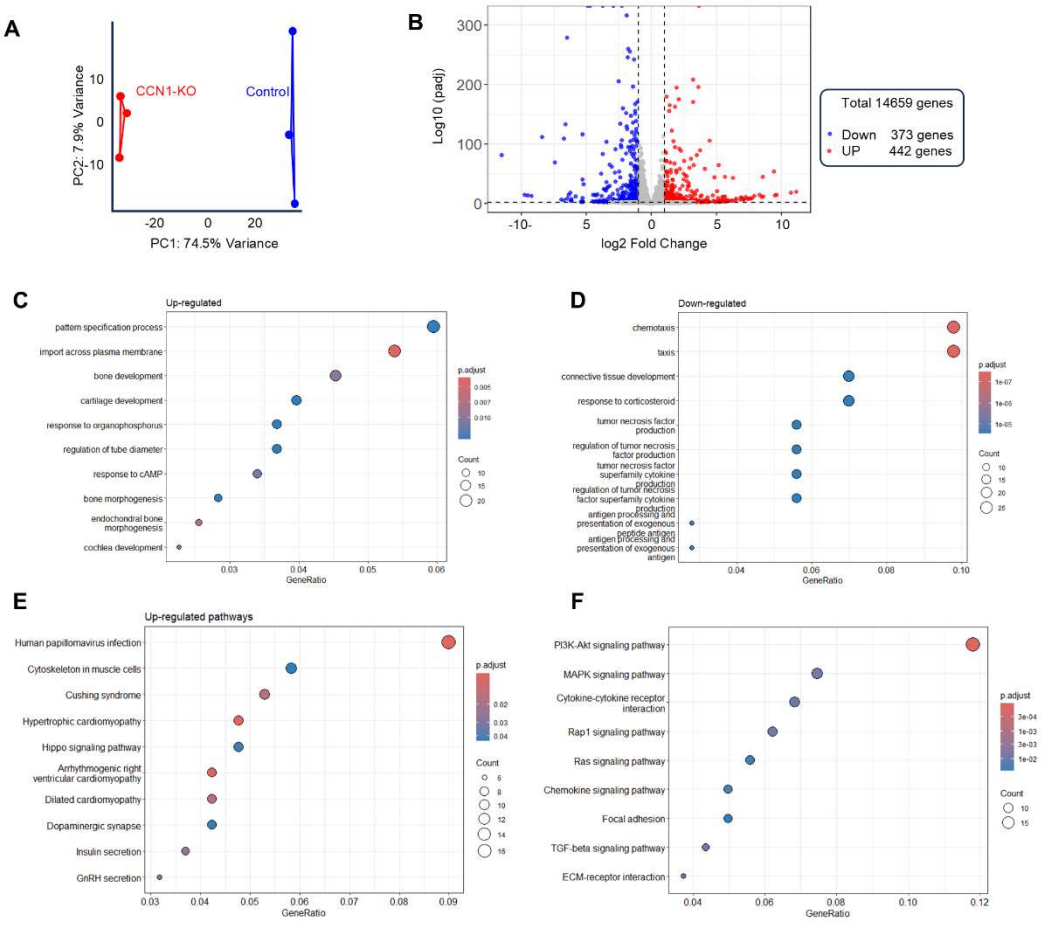


Fig 5 Transcriptomics of CCN1-KO fibroblasts

(A) Principal component analysis (PCA) clustering with samples from control or CCN1-KO NRK49F demonstrated clear divergence. (B) Volcano plot showing a comparison of control of CCN1-KO NRK49F. (C-F) Exhibited the Gene Ontology (GO) analysis of significant differentially expressed genes in Control and CCN1-KO NRK49F (Top 10 up- or downregulated GO terms of biological processes (C, D) and KEGG pathways (E, F)).

Figure 6

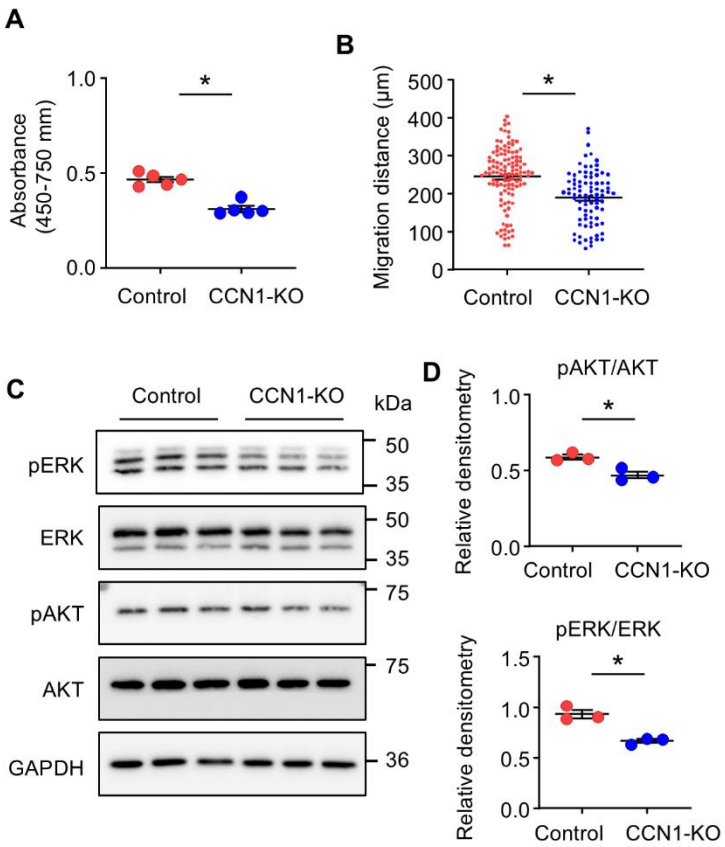


Fig 6 Reduced migration and proliferation in CCN1-KO fibroblasts

(A) Cell proliferation assay data indicated that proliferation was deceased in CCN1-KO NRK49F. (B) Analysis of average endpoint displacements in CCN1-KO NRK49F. (C, D) Western blot analysis of pAKT, AKT, pERK, ERK, and GAPDH in NRK49F (C). The optical densities of bands of pERK and pAKT were normalized against those of ERK and AKT, respectively (D). For all groups, data are means ± SEM. Statistical analyses were performed by paired t-test for comparisons. *P < 0.05.

Figure 7

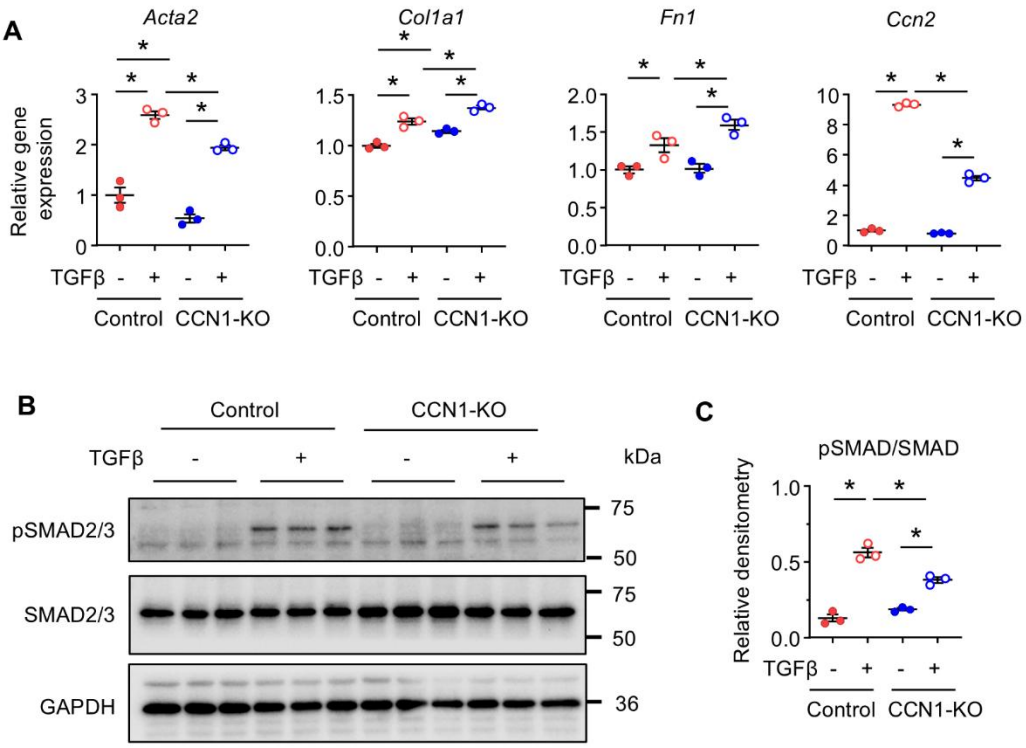


Fig 7 Maladaptive response to TGF-β in CCN1-KO fibroblasts

(A) qPCR of RNA from control or CCN1-KO NRK49F as representative markers of *Acta2*, *Ctgf*, *Co1a1,* and *Fn1*. (B, C) Western blot analysis of pSMAD2/3, SMAD2/3, and GAPDH in NRK49F treated with TGF-β (B). The optical densities of bands of pSMAD2/3 were normalized against SMAD2/3 (C). For all groups, data are means ± SEM. Statistical analyses were performed by ANOVA and Dunnett's post hoc test for comparisons of multiple variables. *P < 0.05.

Supplementary Information

Supplementary Figure S1

Uncropped pictures of gels in Figure 1D

Supplementary Figure S2

Uncropped pictures of gels in Figure 3D

Supplementary Figure S3

Uncropped pictures of membranes in Figure 4C

Supplementary Figure S4

Uncropped pictures of membranes in Figure 6C

Supplementary Figure S5

Uncropped pictures of membranes in Figure 7B

Supplementary Table S1.

Antibodies and reagents for immunofluorescence

Supplementary Table S2.

Antibodies and reagents for Western blotting

Supplementary Table S3.

Primers for RT-qPCR

References

1. Collaborators, G.B.D.C.K.D., *Global, regional, and national burden of chronic kidney disease in adults, 1990-2023, and its attributable risk factors: a systematic analysis for the Global Burden of Disease Study 2023.* Lancet, 2025. 406(10518): p. 2461–2482.
2. Kramann, R., et al., *Matrix Producing Cells in Chronic Kidney Disease: Origin, Regulation, and Activation.* Curr Pathobiol Rep, 2013. 1(4).
3. Duffield, J.S., *Cellular and molecular mechanisms in kidney fibrosis.* J Clin Invest, 2014. 124(6): p. 2299–306.
4. Yamashita, N. and R. Kramann, *Mechanisms of kidney fibrosis and routes towards therapy.* Trends Endocrinol Metab, 2024. 35(1): p. 31–48.
5. Seibt, T., et al., *Mechanisms of regeneration and maladaptive repair in acute kidney injury.* Nat Rev Nephrol, 2026.
6. Qi, R. and C. Yang, *Renal tubular epithelial cells: the neglected mediator of tubulointerstitial fibrosis after injury.* Cell Death Dis, 2018. 9(11): p. 1126.
7. Yang, L., et al., *Epithelial cell cycle arrest in G2/M mediates kidney fibrosis after injury.* Nat Med, 2010. 16(5): p. 535–43, 1p following 143.
8. Liu, B.C., et al., *Renal tubule injury: a driving force toward chronic kidney disease.* Kidney Int, 2018. 93(3): p. 568–579.
9. Gewin, L., R. Zent, and A. Pozzi, *Progression of chronic kidney disease: too much cellular talk causes damage.* Kidney Int, 2017. 91(3): p. 552–560.
10. Tan, R.J., D. Zhou, and Y. Liu, *Signaling Crosstalk between Tubular Epithelial Cells and Interstitial Fibroblasts after Kidney Injury.* Kidney Dis (Basel), 2016. 2(3): p. 136–144.
11. Nakata, T., et al., *Injured tubular epithelia-derived CCN1 promotes the mobilization of fibroblasts toward injury sites after kidney injury.* iScience, 2025. 28(4): p. 112176.
12. Minamida, A., et al., *Injured tubule derived CCN1 exacerbates renal congestion-mediated acute kidney injury and fibrosis.* Sci Rep, 2025. 15(1): p. 20840.
13. Kim, K.H., et al., *The matricellular protein CCN1 in tissue injury repair.* J Cell Commun Signal, 2018. 12(1): p. 273–279.
14. Leask, A., *CCN1: a SASPy protein that plays multifaceted roles in fibrogenesis.* Matrix Biol, 2026. 143: p. 14–17.
15. Kim, K.H., et al., *Matricellular protein CCN1 promotes regression of liver*

fibrosis through induction of cellular senescence in hepatic myofibroblasts. Mol Cell Biol, 2013. 33(10): p. 2078–90.
16. Mooring, M., et al., *Hepatocyte CYR61 polarizes profibrotic macrophages to orchestrate NASH fibrosis.* Sci Transl Med, 2023. 15(715): p. eade3157.
17. Ju, L., et al., *CCN1 promotes hepatic steatosis and inflammation in non-alcoholic steatohepatitis.* Sci Rep, 2020. 10(1): p. 3201.
18. Lai, C.F., et al., *Blockade of cysteine-rich protein 61 attenuates renal inflammation and fibrosis after ischemic kidney injury.* Am J Physiol Renal Physiol, 2014. 307(5): p. F581–92.
19. Sawai, K., et al., *Expression of CCN1 (CYR61) in developing, normal, and diseased human kidney.* Am J Physiol Renal Physiol, 2007. 293(4): p. F1363–72.
20. O'Brien, T.P., et al., *Expression of cyr61, a growth factor-inducible immediate-early gene.* Mol Cell Biol, 1990. 10(7): p. 3569–77.
21. Kusaba, T., et al., *Differentiated kidney epithelial cells repair injured proximal tubule.* Proc Natl Acad Sci U S A, 2014. 111(4): p. 1527–32.
22. Sakuma, H., et al., *Inducible deletion of microRNA activity in kidney mesenchymal cells exacerbates renal fibrosis.* Sci Rep, 2024. 14(1): p. 10963.
23. Kramann, R., et al., *Parabiosis and single-cell RNA sequencing reveal a limited contribution of monocytes to myofibroblasts in kidney fibrosis.* JCI Insight, 2018. 3(9).
24. Yamashita, N., et al., *Cumulative DNA damage by repeated low-dose cisplatin injection promotes the transition of acute to chronic kidney injury in mice.* Sci Rep, 2021. 11(1): p. 20920.
25. Uehara-Watanabe, N., et al., *Proximal tubular epithelia-specific transcriptomics of diabetic mice treated with dapagliflozin.* Heliyon, 2022. 8(9): p. e10615.
26. Li, H., et al., *Comprehensive single-cell transcriptional profiling defines shared and unique epithelial injury responses during kidney fibrosis.* Cell Metab, 2022. 34(12): p. 1977–1998 e9.
27. Lai, C.F., et al., *Cysteine-rich protein 61 plays a proinflammatory role in obstructive kidney fibrosis.* PLoS One, 2013. 8(2): p. e56481.
28. Zhang, N., et al., *Tubule-derived CCN1 drives renal repair via alpha(v)beta(5)-STAT6-ARG1-dependent reprogramming of macrophages.* Cell Death Dis, 2025. 17(1): p. 115.

29. Fischer, A.G., et al., *Matricellular protein CCN1 promotes collagen alignment and scar integrity after myocardial infarction.* Matrix Biol, 2024. 133: p. 14–32.
30. Hu, B.A., et al., *Cardiac fibroblast-derived CCN1 aggravates diabetic cardiomyopathy through ITGAV-ITGB1/integrin alphavbeta1-mediated autophagy inhibition.* Autophagy, 2026. 22(8): p. 1945–1968.
31. Quesnel, K., et al., *CCN1 expression by fibroblasts is required for bleomycin-induced skin fibrosis.* Matrix Biol Plus, 2019. 3: p. 100009.
32. Hutchenreuther, J., et al., *Cancer-associated Fibroblast-specific Expression of the Matricellular Protein CCN1 Coordinates Neovascularization and Stroma Deposition in Melanoma Metastasis.* Cancer Res Commun, 2024. 4(2): p. 556–570.
33. Zhang, F., et al., *The matricellular protein Cyr61 is a key mediator of platelet-derived growth factor-induced cell migration.* J Biol Chem, 2015. 290(13): p. 8232–42.
34. Kurundkar, A.R., et al., *The matricellular protein CCN1 enhances TGF-beta1/SMAD3-dependent profibrotic signaling in fibroblasts and contributes to fibrogenic responses to lung injury.* FASEB J, 2016. 30(6): p. 2135–50.
35. Finnson, K.W., Y. Almadani, and A. Philip, *Non-canonical (non-SMAD2/3) TGF-beta signaling in fibrosis: Mechanisms and targets.* Semin Cell Dev Biol, 2020. 101: p. 115–122.
36. Hsu, P.L., et al., *Shear-Induced CCN1 Promotes Atheroprone Endothelial Phenotypes and Atherosclerosis.* Circulation, 2019. 139(25): p. 2877–2891.
37. Leu, S.J., S.C. Lam, and L.F. Lau, *Pro-angiogenic activities of CYR61 (CCN1) mediated through integrins alphavbeta3 and alpha6beta1 in human umbilical vein endothelial cells.* J Biol Chem, 2002. 277(48): p. 46248–55.
38. Lee, H.Y., et al., *Forkhead transcription factor FOXO3a is a negative regulator of angiogenic immediate early gene CYR61, leading to inhibition of vascular smooth muscle cell proliferation and neointimal hyperplasia.* Circ Res, 2007. 100(3): p. 372–80.
39. Emre, Y. and B.A. Imhof, *Matricellular protein CCN1/CYR61: a new player in inflammation and leukocyte trafficking.* Semin Immunopathol, 2014. 36(2): p. 253–9.

753

Supplementary Files

This is a list of supplementary files associated with this preprint. Click to download.

- 20261010FibroCCN1Suppl.docx